JOURNAL OF MATERIALS SCIENCE 28 (1993) 5759–5764

Mechanical properties of Zr–3Sn–1Mo–1Nb alloy at various temperatures

R. KRÁL, P. LUKÁČ, Z. TROJANOVÁ, F. KRÁL
Department of Metal Physics, Charles University Prague, Ke Karlovu 5, 121 16 Prague 2, Czechoslovakia

The deformation characteristics of Zr–3Sn–1Mo–1Nb alloy have been investigated by tensile testing in the temperature range 300–1000 K at a constant crosshead speed corresponding to the strain rate of $6.7 \times 10^{-5} s^{-1}$. At lower temperatures, below about 500 K, the flow stress of the sample decreased with increasing temperature, whereas an inverse temperature dependence of the yield stress was found at temperatures between 500 and 700 K. At higher temperatures, above 700 K, the normal dependence of the yield stress on temperature was again observed. The maximum stress exhibited a similar temperature dependence. At higher temperature, serrations were found on the flow stress curves at the very beginning of deformation. The main deformation mechanisms are assumed to be a locking–unlocking mechanism connected with cross-slipping.

1. Introduction

The objective of many studies of the mechanical properties of alloys is to find the relation between stress and strain at various temperatures. Zirconium alloys have found wide high-temperature applications in the nuclear and chemical industry owing to their good mechanical properties and their corrosion resistance. The alloy constitution and thermal treatment may contribute to stabilization and solid solution as well as precipitation strengthening. Some elements, such as tin, molybdenum and niobium, are often added to improve high-temperature properties. The influence of chemical composition, especially additions of tin, molybdenum and niobium, on creep characteristics of martensitic zirconium alloys has been extensively investigated at temperatures between 623 and 823 K by Pahutová *et al.* [1–10]. They reported [3, 10] that the steady state creep rate of the quaternary Zr–3% Sn–1% Mo–1% Nb (nominal composition in wt %) alloy is some orders of magnitude lower than that of α-zirconium. According to Pahutová *et al.* [10] an athermal deformation mechanism contributes to the measured creep rates at the highest applied stress.

In the present work the tensile properties of the Zr–3% Sn–1% Mo–1% Nb samples were investigated at various temperatures between 300 and 1000 K.

2. Experimental procedure

The material used in this investigation was the quaternary alloy of nominal composition Zr–3% Sn–1% Mo–1% Nb (in wt %). Chemical analysis showed the actual elemental composition to be 2.8 wt % Sn, 0.91 wt % Mo, 0.94 wt % Nb. and 430 p.p.m. O_2.

A more detailed description of material preparation is given elsewhere [3]. The main grain size was determined by the linear intercept method to be 0.33 mm, the grains being rather equiaxed. The test specimens were cut from a thin plate in such a way to be parallel to the rolling direction. The specimens had a gauge length of 50 mm and a rectangular cross-section 3.3 $\times$ 2.5 mm^2. Each specimen was quenched in water from temperatures about 10 K higher than the equilibrium temperature $(\alpha + \beta)/\beta$ and then annealed for 8 h at 823 K. The alloy exhibits the hexagonal martensitic structure.

The tensile tests were carried out in an Instron tensile machine (Type 1186) with a constant crosshead speed which corresponded to an initial strain rate of $6.67 \times 10^{-5} s^{-1}$ at two temperatures (450 and 800 K); the initial strain rates ranged between 6.67×10^{-5} and $6.67 \times 10^{-3} s^{-1}$. A furnace with a dynamic argon atmosphere was used for the test temperatures higher than room temperature. The specimens were inserted into the furnace at room temperature and kept for 40 min at the deformation temperature before testing. Immediately after the test the furnace was opened and the specimen was cooled down. During the tests the temperatures were controlled to within ± 2 °C. The tests were conducted at various temperatures between room temperature and 1000 K.

After the test, the specimens were prepared for microstructural observations using both optical and transmission electron microscopy (TEM). The specimens for metallographic examination were prepared by polishing in a solution containing 10% HNO_3, 20% HF and 70% glycerin for 150 s at 20 °C. A Neophot 21 microscope was used.

For the observation of the dislocation microstructure, a Jeol 2000 FX operating at 200 kV was used. Thin foils for TEM were prepared after the test by mechanical grinding and then electropolishing using a twin-jet thinner Tenupol 2 and a solution of 5.3 g LiCl,

0022–2461

11.2 g $Mg(ClO_4)_2$, 150 ml butylcellosolve and 750 ml methanol under 100 V and 80 mA at $-65\,^{\circ}C$ until perforation occurred.

3. Results

The microstructure of the specimen before tensile testing is shown in Fig. 1 using both optical and transmission electron microscopy. In addition to fine precipitates, the lamelar structure can be seen. Pahutová *et al.* [3, 5, 9] have observed the phase β_{Nb}, and $ZrMo_2$ and Zr_4Sn secondary phases dispersed in the quaternary Zr–Sn–Mo–Nb alloy. Transmission electron micrographs showed the same microstructure as observed by Pahutová *et al.* [3, 5, 9].

Typical examples of the true stress, σ, versus true strain, ε, curves obtained by the tension test at various temperatures at the strain rate of $6.67 \times 10^{-5}\,s^{-1}$ are shown in Fig. 2. It is seen that the flow stress gradually decreases with increasing deformation temperature with the exception of the temperature range about 500–700 K where the flow stress increases with increasing temperature. Two different shapes of the stress–strain curves may be identified depending on the test temperature. The samples deformed at temperatures lower than 700 K exhibit parabolic strain hardening, whereas those deformed at temperatures higher than 800 K exhibit a tendency towards the steady state flow behaviour.

In accordance with such a characterization of the deformation behaviour, typical features may be found in the temperature dependence of the 0.2% offset yield stress, σ_{02}, and the maximum stress, σ_{max}. The values of σ_{02} and σ_{max} are plotted as a function of the test temperature in Fig. 3. It is seen that at low temperatures, σ_{02} as well as the maximum stress decrease with increasing temperature, reaching a local minimum at about 500 K, then in the intermediate temperature range from above 500–700 K, the inverse temperature dependence of the flow stress appears, i.e. both σ_{02} and σ_{max} increase with increasing temperature. At temperatures higher than 700 K, the flow stress decreases very strongly with increasing temperature; from about 690 and 720 MPa at 700 K to 58 and 92 MPa at 1000 K for σ_{02} and σ_{max}, respectively. The difference between σ_{max} and σ_{02} is very small at temperatures higher than 700 K.

In Fig. 3, the variation of σ_s with the test temperature is also given. σ_s is the characteristic of quasi-steady state deformation behaviour (saturation) and it was obtained by the extrapolation of the stress dependence of the work-hardening rate to zero stress [11] assuming a balance between immobilization and annihilation of dislocations. The calculated values of σ_s according to three different models [12–14] are very close to experimentally determined values of σ_{max} which is expected, due o the shapes of the stress–strain curves (see Fig. 1).

Fig. 4 shows the relation between the fracture elongation, δ, and the test temperature. At temperature lower than 700 K the elongation changes non-monotonically with increasing temperature. The elongation reaches a minimum value, $\delta = 1.9\%$, at

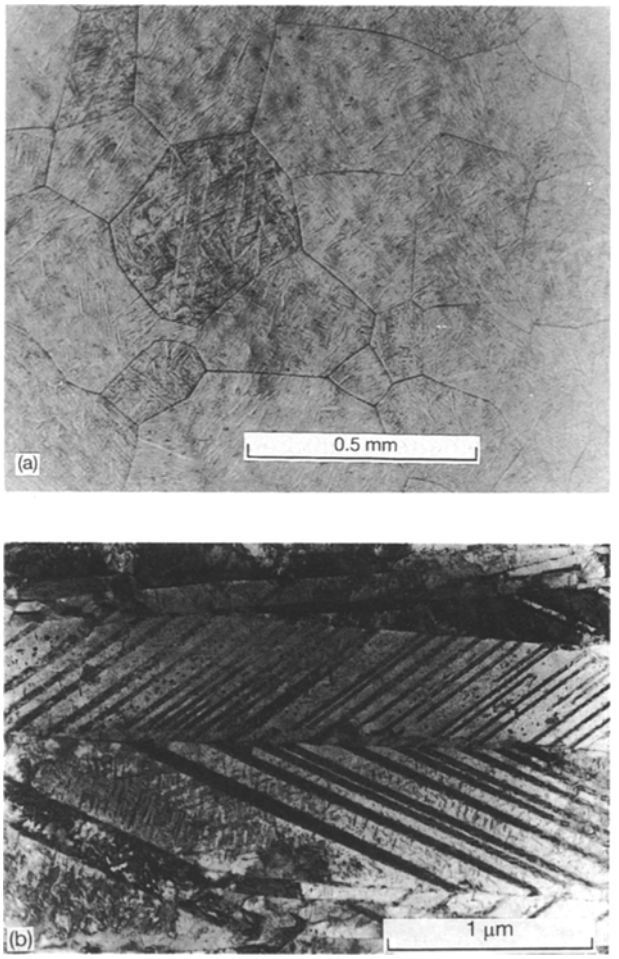

Figure 1 (a) Microstructure of the specimen before tensile testing. (b) Transmission electron micrograph of the specimen before testing.

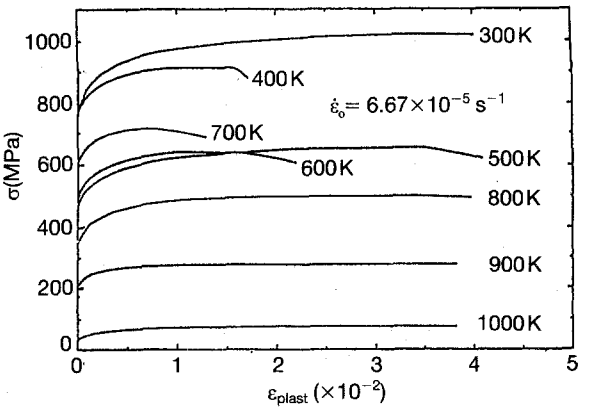

Figure 2 Flow curves for Zr–3Sn–1Mo–1Nb alloy obtained by tensile testing at various temperatures at a strain rate of $6.67 \times 10^{-5}\,s^{-1}$.

400 K. At temperatures higher than 700 K, the elongation increases with increasing temperature, reaching a large elongation, about 38%, at 950 K.

It is interesting to note that serrations on the flow curves are observed at the very beginning of deformation (in the transition between elastic and plastic deformation) at temperatures higher than 850 K. A typical example is shown in Fig. 5. The serrated flow may be characterized by parameters shown in Fig. 5: the flow stress at the onset of serrations, σ_i, the stress amplitude of serrations, $\Delta\sigma$, and the strain interval, δ_c,

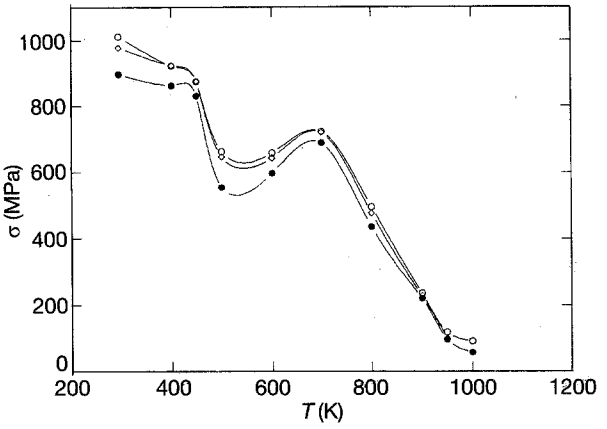

Figure 3 (●) 0.2% offset yield stress, σ_{02}, (◇) saturation stress, σ_s, and (○) the maximum stress, σ_{max}, of Zr–3Sn–1Mo–1Nb alloy as a function of the deformation temperature; strain rate = $6.67 \times 10^{-5} s^{-1}$.

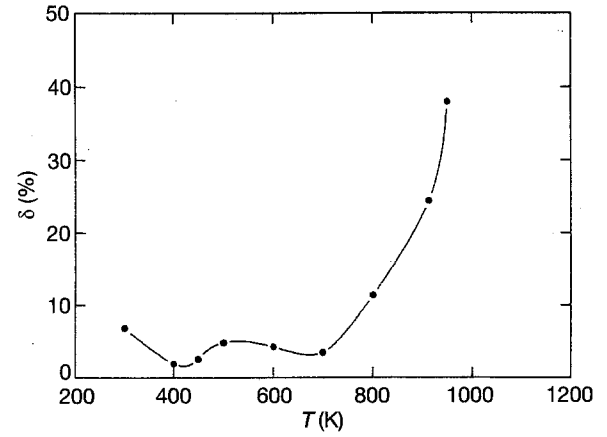

Figure 4 Temperature dependence of fracture elongation, δ, for Zr–3Sn–1Mo–1Nb alloy. $\dot{\varepsilon}_0 = 6.67 \times 10^{-5} s^{-1}$.

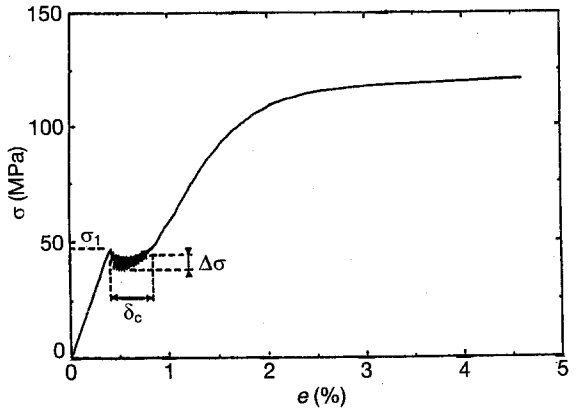

Figure 5 A typical example of serrations on the flow curve; parameters of serrations are indicated. $\dot{\varepsilon}_0 = 6.67 \times 10^{-5} s^{-1}$.

in which serrations appear. All the parameters above mentioned exhibit a non-monotonic temperature variation (Fig. 6). The values of σ_i, $\Delta\sigma$ and δ_c have been found to be in the ranges between 43 and 84 MPa, 4 and 10 MPa, and 0.1% and 0.75%, respectively. Extreme values $\sigma_i = 140$ MPa, $\Delta\sigma = 108$ MPa, and $\delta_c = 2.4\%$ have been measured at 913 K. These serrations may be caused by the phenomenon of mechanical twinning. The serrations in the load–elongation curve may be a result of the motion of partial dislocations across various slip planes.

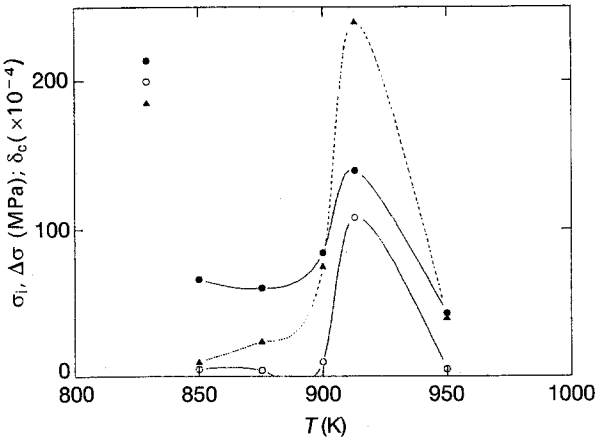

Figure 6 Effect of temperature on the serrations parameters. (●)σ_i, (○) $\Delta\sigma$, (▲) δ_c. $\dot{\varepsilon}_0 = 6.67 \times 10^{-5} s^{-1}$.

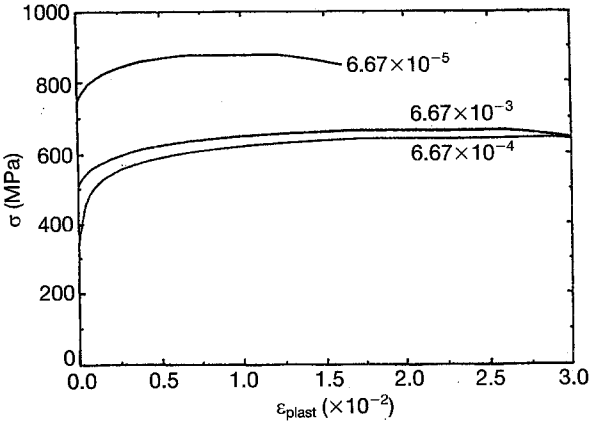

Figure 7 Flow curves for Zr–3Sn–1Mo–1Nb alloy at 450 K at three different strain rates.

4. Discussion

The temperature range between 300 and 700 K may be characterized by a non-monotonic temperature dependence of the flow stress. In addition, the strain-rate dependence of the flow stress is also non-monotonic. Fig. 7 shows the stress–strain curves obtained at different strain rates at 450 K. It is seen that the flow stress decreases when the strain rate is increased to $6.67 \times 10^{-4} s^{-1}$. The existence of a hump in the temperature of the flow stress could be explained assuming that dynamic strain ageing occurs. Accordingly, the occurrence of the serrated flow could be observed as a result of unlocking of aged dislocation from the atmospheres of clusters of solute atoms. The strength of the locking due to the solute atmospheres should increase with increasing temperature and it should result in the inverse temperature dependence of the flow stress, on the one hand, and in the serrations on the flow curves, on the other. However, no serrated flow has been observed in this work at temperatures lower than 700 K. We can conclude that dynamic strain ageing is not responsible for the increase of the flow stress with increasing temperature.

We may assume that the anomalous increase in the flow stress with increasing temperature in the range 450–700 K could be caused by the operating dislocation mechanism.

In accordance with observations on zirconium [15] and its alloys (e.g. [16]), slip occurs on the $\{1\,0\,\bar{1}\,0\}$ prismatic planes. Glide of ***a***-dislocations, that is with the Burger's vector $\boldsymbol{b} = \frac{1}{3}\langle 1\,1\,\bar{2}\,0\rangle$, plays an important role. During deformation of polycrystals, and single crystals with suitable orientation of the tensile axis, not only prismatic slip but also the slip on pyramidal planes $\{1\,0\,\bar{1}\,1\}$ and/or $\{1\,1\,\bar{2}\,\bar{2}\}$ may be an active deformation mode [17]. In this case, slip in the $\langle 1\,1\,\bar{2}\,3\rangle$ direction, i.e. the motion of $(\boldsymbol{a} + \boldsymbol{c})$ dislocations (with the Burgers vector $\boldsymbol{b} = \frac{1}{3}\langle 1\,1\,\bar{2}\,3\rangle$) is assumed.

We can assume that screw ***a***-dislocations in the zirconium alloys, as first proposed by Naka et al. [18, 19], may split in a nonplanar manner into two partials lying on the prismatic plane and two partials lying on the first-pyramidal planes $(1\,0\,\bar{1}\,1)$ and $(1\,0\,\bar{1}\,\bar{1})$, respectively. According to Vítek and Igarashi [20], the cores of the partial dislocations on prismatic plane are non-planar. The **a** screw dislocations take alternately two configurations corresponding to two states of the core structure: a glissile configuration and a sessile. According to a model proposed by Naka *et al.* [19] the dislocations move by a succession of thermally activated sessile-glissile transitions. This is in agreement with the experimental results obtained by Couret and Caillard [21, 22] investigating prismatic glide in beryllium. They have also shown that screw dislocations may cross-slip between basal and prismatic planes during deformation and have proposed a locking–unlocking mechanism [21–24]. Unlocking is cross-slip to a plane of higher energy, and locking corresponds to the second cross-slip process from a plane of higher energy to that of lower energy. Screw dislocations in the metastable glissile core configuration may glide freely over some distance and then they are locked again. If temperature increases, the probability of locking increases and thus an increase in the stress is necessary to recombine a spread screw dislocation. It means that cross-slipping becomes more difficult with increasing temperature and this would correspond to an increase of the flow stress with increasing temperature, which is observed in a certain temperature range. Hence we may assume that the inverse temperature dependence of the flow stress (the strength anomaly) is controlled by the locking–unlocking mechanism [21–24]. The slip mechanism of $(\boldsymbol{a} + \boldsymbol{c})$-dislocations on a prism plane may also cause a strongly negative temperature dependence of the flow stress [25].

At temperatures higher than 700 K, the yield stress as well as the maximum stress decrease very strongly with increasing temperature and a steady state flow behaviour is typical. The flow stress increases with increasing strain rate at 800 K as shown in Fig. 8. From the slope of the least squares plot of log σ_{02} against log $\dot{\varepsilon}$, the stress exponent in the equation $\dot{\varepsilon} = A\sigma^n$ (where A is a constant) is calculated to be 12 ± 2. If we assume that the following equation for high temperature creep

$$\dot{\varepsilon} = A(\sigma/G)^n \exp(-Q/RT) \qquad (1)$$

where G is the shear modulus and R is the gas

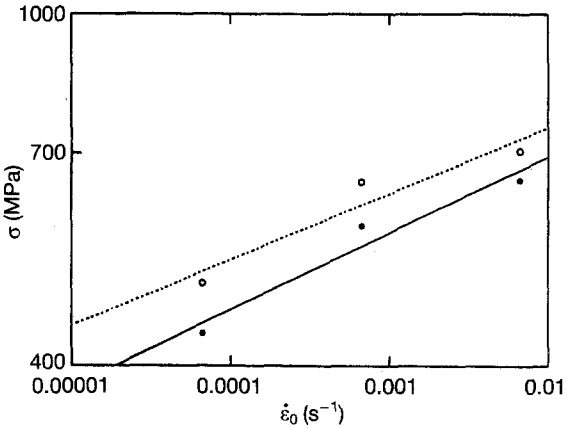

Figure 8 Strain-rate dependence of the (●) flow stress, σ_{02}, and (○) the maximum stress, σ_{max}, at 800 K.

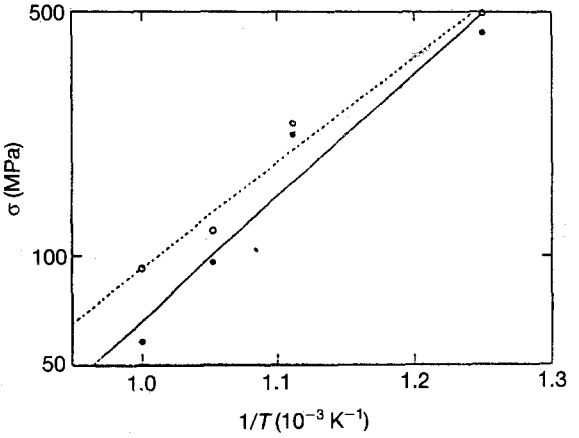

Figure 9 Arrhenius plot of the temperature dependence of (●) the flow stress, σ_{02}, and (○) the maximum stress, σ_{max}, at temperatures higher than 700 K. $\dot{\varepsilon}_0 = 6.67 \times 10^{-5}\,s^{-1}$.

constant, may be applicable for the present results, an apparent activation energy, Q, may be determined. Using the above estimated value of the stress exponent, the Arrhenius plot of the temperature dependence of the flow stress, shown in Fig. 9 gives an apparent activation energy for deformation of 340 KJ mol^{-1}.

In this case, the dislocation structure may not vary and we may consider that the deformation mechanism does not depend on the microstructure.

The feature of the tensile behaviour at a constant strain at higher temperatures presented in this work is very close to that obtained in creep experiments by Pahutová *et al.* [3, 10]. We can compare our results with those obtained by Pahutová *et al.* [3] measured in the temperature range 623 and 823 K and for the stresses between 40 and 750 MPa. From their measurements [3] of steady-state creep rate, $\dot{\varepsilon}$, as a function of the applied stress, σ, one can deduce that the parameter of the stress sensitivity of steady-state creep rate defined as

$$n = \left(\frac{\partial \ln \dot{\varepsilon}}{\partial \ln \sigma}\right)_T \qquad (2)$$

increases with increasing stress level imposed from values close to 3 up to values of 7–10 and for higher temperature, n is higher than 10. It is interesting to

note two points: (a) at 623 K the obtained steady-state creep rates have values between 10^{-10} and $10^{-9}\,s^{-1}$ and from their plot of log $\dot{\varepsilon}$ against log σ one may estimate that n is negative, which corresponds to the inverse temperature dependence of the flow stress measured in this work; (b) the values of the applied stress at which the steady-state creep rate is about $6 \times 10^{-5}\,s^{-1}$, are very close to the values of the flow stress determined in tension at the strain rate $6 \times 10^{-5}\,s^{-1}$. Pahutová *et al.* [3] have estimated the apparent activation energy for the steady-state creep to be in the range between 213 and 410 K kJ mol^{-1}. We may, therefore, conclude that the correlation between tensile properties obtained in creep and at constant strain rate for the same conditions is very good.

The observed strain-hardening rate for samples deformed at temperatures higher than 700 K is close to zero, which is a result of a dynamic balance between hardening and softening mechanisms. At these higher temperatures also the motion of dislocations in the pyramidal slip systems should be expected. Interaction between dislocations in the second pyramidal slip systems can take place according to the following dislocation reaction

$$\tfrac{1}{3}[1\,1\,\bar{2}\,\bar{3}] + \tfrac{1}{3}[\bar{2}\,1\,1\,3] \rightarrow \tfrac{1}{3}[\bar{1}\,2\,\bar{1}\,0] \qquad (3)$$

This dislocation reaction can result in softening and cause the quasi-steady state course of the observed flow stress. It is likely that the more the pyramidal $(a + c)$ dislocations that are moving, the higher the probability Reaction 1 has. The number of the moving $(a + c)$-dislocations depends on the temperature of deformation: the higher the temperature the greater the number of dislocations that are in motion.

It should be mentioned also that at temperatures higher than 700 K, cross-slip of screw dislocations takes place. The cross-slipped dislocations can interact with the dislocations present in the cross-slip plane and the dislocation annihilation can occur. Both mechanisms, i.e. the dislocation reaction among $(a + c)$-dislocations and the cross-slip, as well as the annihilation, can result in a decrease of strain-hardening rate, which is observed.

At temperatures higher than 800 K, serrations begin at the very onset of plastic flow. These serrations may be caused by the formation of mechanical twins. Mechanical twinning is an important mode of deformation in hexagonal metals and one may expect that mechanical twinning in a quaternary alloy with a complex microstructure, including twins due to diffusionless transformation, may be influenced by temperature. Westlake [26] has presented models for the dislocation mechanism of twinning in zirconium. An analysis of different dislocation reactions in prismatic and pyramidal slip systems has shown the existence of a twin dislocation on the twinning plane $(\bar{1}\,0\,1\,2)$ with the Burgers vector in the twinning direction $[1\,0\,\bar{1}\,1]$. The dislocation reaction has the following form

$$\tfrac{1}{3}[2\,\bar{1}\,\bar{1}\,0]_{(0\,1\,\bar{1}\,0)} + \tfrac{1}{3}[1\,1\,\bar{2}\,3]_{(\bar{1}\,\bar{1}\,2\,2)} \rightarrow [1\,0\,\bar{1}\,1]_{(\bar{1}\,0\,1\,2)} \qquad (4)$$

We may assume that pile-ups of dislocations in prismatic and pyramidal slip systems are formed under thermomechanical treatment. The local stress at the tip of the pile-up may be high enough to nucleate a twin and then to induce the formation and growth of twins. One may expect that mechanical twinning in the quaternary alloy with a complex microstructure including twins created during the diffusionless transformation, may be influenced by temperature. According to our knowledge it is not obvious whether there exists a critical stress for the formation of deformation twins, and what the temperature dependence of this stress may be.

5. Conclusions

In order to investigate tensile properties of Zr–3Sn–1Mo–1Nb alloy, tensile tests were carried out under various temperatures at a constant strain rate of the order $10^{-5}\,s^{-1}$. It was found that at temperatures below about 500 K the flow stress decreases with increasing temperature, whereas the yield stress increases with increasing temperatures in the temperature range 500–700 K. At temperatures higher than 700 K the flow stress decreases with increasing temperature. The observed flow behaviour may be explained by assuming a locking–unlocking mechanism connected with cross-slip.

Acknowledgements

The authors thank Professor Čadek and Dr M. Pahutová, Institute of Physical Metallurgy, Czechoslovak Academy of Sciences, Brno, for the supply of samples, and Dr B. Smola and Dr J. Pešička, Department of Metal Physics, Charles University, Prague, for their assistance in TEM studies.

References

1. M. PAHUTOVÁ, V. ČERNÝ and J. ČADEK, *Metall. Mater.* **13** (1975) 417.
2. *Idem, ibid.* **14** (1976) 252.
3. M. PAHUTOVÁ, K. KUCHAŘOVÁ and J. ČADEK, *ibid.* **14** (1976) 567.
4. *Idem, ibid.* **14** (1976) 702.
5. *Idem, Mater. Sci. Eng.* **27** (1977) 239.
6. *Idem. ibid.* **27** (1977) 249.
7. M. PAHUTOVÁ and J. ČADEK, *ibid.* **20** (1975) 277.
8. M. PAHUTOVÁ, J. ČADEK and V. ČERNÝ, *J. Nucl. Mater.* **67** (1976) 285.
9. *Idem, ibid.* **68** (1977) 111.
10. M. PAHUTOVÁ, K. KUCHAŘOVÁ and J. ČADEK, *ibid.* **131** (1985) 20.
11. R. KRÁL, Diploma Thesis, Charles University (1992).
12. U. F. KOCKS, *J. Eng. Mater. Tech. (ASME) H* **98** (1976) 76.
13. Y. ESTRIN and H. MECKING, *Acta Metall.* **32** (1984) 57.
14. W. ROBERTS, in "Deformation, Processing, and Structure" edited by C. Krausz (ASM Metals Park, 1984) p. 109.
15. J. E. BAILEY, *J. Nucl. Mater.* **3** (1962) 300.
16. I. ARMAS and M. BOČEK, *ibid.* **115** (1983) 263.
17. J. P. HIRTH and J. LOTHE, "Theory of Dislocation" (Wiley, New York, 1982).
18. S. NAKA and A. LASALMONIE, *J. Mater. Sci.* **18** (1983) 2613.

19. S. NAKA, A. LASALMONIE, P. COSTA and L. P. KUBIN, *Philos. Mag.* **A57** (1988) 717.
20. M. VÍTEK and M. IGARASHI, *ibid.* **A63** (1991) 1059.
21. A. COURET and D. CAILLARD, *ibid.* **A59** (1989) 783.
22. *Idem, ibid.* **A59** (1989) 801.
23. *Idem, ibid.* **A63** (1991) 1045.
24. *Idem, J. Phys. III* **1** (1991) 885.
25. H. NUMAKURA, Y. MINONISHI and M. KOIWA, *Philos. Mag.* **A63** (1991) 1077.
26. D. G. WESTLAKE, *Acta Metall.* **9** (1961) 327.

Received 28 May 1992
and accepted 16 March 1993